Semi-Automatic Analysis of Gyrotropic Semiconductor Waveguides Using Neural Network

D. Plonis*, V. Malisauskas and A. Serackis

Department of Electronic Systems, Vilnius Gediminas Technical University (VGTU)

Naugarduko str., 41-425, LT-03227 Vilnius, Lithuania

This paper focuses on the analysis technique of gyrotropic circular cylindrical semiconductor waveguide by the use of an electrodynamical model. Authors propose the semi-automatic extraction of the dispersion characteristics by the use of single-layer perceptron neural network. The waveguide analysis algorithm consists of four main stages: initialization of system parameters, evaluation of transcendental linear dispersion equation system, extraction of dispersion characteristics and evaluation of the waveguide broad bandwidth. In this paper three types of waveguides (n-InP, n-InSb and p-InP) are analysed using a proposed algorithm. According to the results of analysis, the use of gyrotropic n-InP and p-InP semiconductor, semiconductor–dielectric waveguides are more preferred than to n-InSb waveguides due to their wider broad bandwidth.

PACS: 84.40.Az, 07.05.Mh

1. Introduction

In super high frequencies there are often used circular cylindrical waveguides. These types of waveguides were investigated in early 1947. Due to the growing interest in equipment for super high frequency signals, the analysis of circular cylindrical waveguides is relevant. Various materials could be selected for these waveguides considering the diameter of the waveguide, which depends on the specific application of waveguide. The gyrotropic semiconductor and semiconductor–dielectric waveguides are analysed in this paper.

Comparison between electrodynamical characteristics and gyrotropic ferrite waveguides has proved that these waveguides are relevant tools, especially nowadays. Before designing any waveguide with diameter below 2 mm the selection of right material is very important. The material, selected for the waveguide, influences its electrodynamical characteristics. Therefore, the electrodynamical analysis of the waveguides, designed for the use in various microwave devices is essential [1–5].

Two main parameters have to be estimated for the designed waveguide: broad bandwidth and working frequency range. Analysis of the dispersion characteristics for specific waveguide enables to retrieve the broad bandwidth for the analysed waveguide design. These characteristics are usually achieved using numerical analysis methods: finite-difference time-domain, finite element, moments or boundary element, singular integral equation [6–9]. As an alternative to these waveguide analysis methods, the mathematical model for analytical analysis of the waveguides is proposed in the previous works of authors [10–14]. The use of analytical method suggested by authors leads to more accurate results in estimation of waveguide broad bandwidth.

In this paper three types of gyrotropic cylindrical circular waveguides are analysed: n-InP, n-InSb and p-InP. The extraction of the dispersion characteristics requires classification of nodes, calculated by the use of mathematical model for the gyrotropic waveguide. Further approximation of the nodes, belonging to the same class, is necessary for the estimation of the gyrotropic waveguide broad bandwidth.

Various intelligent systems can quickly solve data analysis [15–18]. In this paper a single-layer perceptron (SLP) neural network (NN) is used for the classification of different circular gyrotropic cylindrical waveguide nodes. The dispersion characteristics are received by approximating extracted nodes, belonging to the same mode of the waveguide.

2. Basics of gyrotropic semiconductor waveguides

General structure of the gyrotropic open circular cylindrical semiconductor and semiconductor–dielectric waveguide is shown in Fig. 1. The electrodynamical model for this kind of waveguide is presented in literature [13, 19] and is suitable for ferrite, semiconductor, dielectrical, gas discharge, and optical waveguide analysis.

In this paper the gyrotropic waveguides with the semiconductor core, exposed by a constant longitudinal magnetic field, defined as magnetic flux density vector $\boldsymbol{B}_0$

* corresponding author; e-mail: darius.plonis@el.vgtu.lt

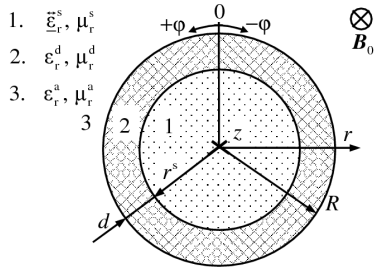

Fig. 1. General structure of the gyrotropic open circular cylindrical semiconductor and semiconductor–dielectric waveguide: 1 — semiconductor core, 2 — external non-magnetic dielectric layer, 3 — air.

(see Fig. 1), are analysed. The core of the waveguide is characterized by the complex permittivity tensor $\overleftrightarrow{\varepsilon}_{\rm r}^{\rm s}$ and the real relative permeability $\mu_{\rm r}^{\rm s} = 1$.

Semiconductor complex relative permittivity tensor is used to calculate the coefficients of waves transversals — $k_{\perp 1,2}^{\rm s}$. These coefficients are used for the evaluation of complex determinant elements $\boldsymbol{a}_{jk}$ [14, 19]. The tensor is presented as [13, 20]:

$$\overleftrightarrow{\varepsilon}_{\rm r}^{\rm s} = \begin{vmatrix} \varepsilon_{xx}^{\rm s} & {\rm i}\varepsilon_{xy}^{\rm s} & 0 \\ -{\rm i}\varepsilon_{xy}^{\rm s} & \varepsilon_{xx}^{\rm s} & 0 \\ 0 & 0 & \varepsilon_{zz}^{\rm s} \end{vmatrix}, \tag{1}$$

where $\varepsilon_{xx}^{\rm s}, \varepsilon_{xy}^{\rm s}, \varepsilon_{zz}^{\rm s}$ are complex elements of the tensor.

In the analysed waveguide model a non-magnetic dielectric layer surrounds the core of the waveguide (a second model area in Fig. 1) and is characterized by the real relative permittivity $\varepsilon_{\rm r}^{\rm d}$ and the real relative permeability $\mu_{\rm r}^{\rm d} = 1$. The environment of the analysed waveguide in the model is air with permittivity and permeability $\varepsilon_{\rm r}^{\rm a} = \mu_{\rm r}^{\rm a} \approx 1$.

The detailed description for the mathematical model of the open gyrotropic cylindrical semiconductor waveguide can be found in the literature [13, 19].

The gyrotropic semiconductor waveguides dispersion equations can be solved by the use of Maxwell's equations presented in [13, 14]. The transcendental linear dispersion equation system of the 8th order determinant for open circular cylindrical semiconductor waveguides with external dielectric layer is expressed by $D^{\rm s} = \det[\boldsymbol{a}_{jk}] = 0$, where j is a column and k is a row index of determinant. The non-zero complex determinant elements are presented in [13]. Solving the dispersion equation, the phase characteristics of the modes and other electrodynamics parameters are obtained.

3. Gyrotropic waveguides dispersion characteristics analysis algorithm

The gyrotropic waveguide analysis algorithm proposed in this paper (algorithm 1) is divided into four stages: (A) initialization of system parameters; (B) evaluation of transcendental linear dispersion equation system; (C) extraction of dispersion characteristics; in assistance of single-layer perceptron NN and (D) evaluation of the waveguide broad bandwidth for the analysed waveguide.

The evaluation of coefficients in the 1st step of the algorithm B stage (algorithm 1) is performed using equations presented in [13]. The extraction of waveguide dispersion characteristics is performed by a two SLP NN. The design of the SLP NN depends on the number of dispersion characteristics which are necessary to be extracted

$$n_{\rm ch} = 2^{n_{\rm L}}, \tag{2}$$

where $n_{\rm L}$ is the number of neurons for SLP NN. The extraction of dispersion characteristics is presented by using two outputs of the SLP NN and three waveguide modes are separated from each other.

The output of the SLP NN (shown in Fig. 2) for the extraction of three dispersion characteristics can be defined as follows:

$$\begin{cases} y_1 = \Phi\left(w_{11} f r_t^{\rm s} + w_{12} h' r_t^{\rm s} + b_1\right), \\ y_2 = \Phi\left(w_{21} f r_t^{\rm s} + w_{22} h' r_t^{\rm s} + b_2\right), \end{cases} \tag{3}$$

where $\Phi(x)$ is a hard limiting SLP activation function, w_{ij} are the weights of the i-th neuron for the j-th input of the SLP, $b_{1,2}$ are the biases of 1 and 2 neuron respectively, $fr_t^{\rm s}$ is a normalized frequency, $h' r_t^{\rm s}$ is a normalized phase constant and t is a number of iteration.

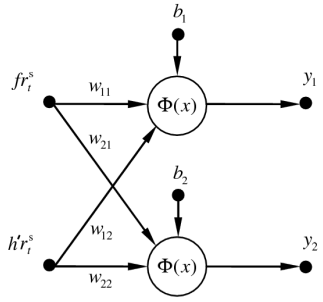

Fig. 2. Structure of the single-layer perceptron neural network.

The SLP NN training is performed by generating random initial weights w_{ij} (Fig. 2) and putting the $fr_t^{\rm s}$ and $h' r_t^{\rm s}$ as the inputs of the network and y_1, y_2 as the desired outputs. The hard limiting function is selected as an activation function for the both neurons. The update of weights is performed in accordance to an error received for the given SLP NN inputs using gradient descent learning. Each data class requires to set at least two points for training.

Algorithm 1. Dispersion characteristics analysis algorithm of the gyrotropic waveguides

A. Initialization of system parameters. $\varepsilon_{\rm r}^{\rm d}$, $\varepsilon_k^{\rm sn,p}$, m, m^*, $f_{\min}$, $f_{\max}$, Δf, $h'_{\min}$, $h'_{\max}$, $\Delta h'$, B_0, μ, N, R, $r^{\rm s}$.

B. Evaluation of transcendental linear dispersion equation system.

for $f \to f_{\min}$, Δf, $f_{\max}$ **do**

1) Evaluation of the coefficients [13]: $\mathrm{Re}(\boldsymbol{\varepsilon}^{\mathrm{s}}_{xx}, \boldsymbol{\varepsilon}^{\mathrm{s}}_{xy}, \boldsymbol{\varepsilon}^{\mathrm{s}}_{zz})$, $\boldsymbol{\varepsilon}_{\mathrm{ef}}$, $\boldsymbol{\mu}_{\mathrm{ef}}$, $\boldsymbol{\Delta}_{\mathrm{S}}$, k, $\boldsymbol{k}^{\mathrm{s}}_{\perp 1,2}$, $\boldsymbol{k}^{\mathrm{a}}_{\perp}$, $\boldsymbol{k}^{\mathrm{d}}_{\perp}$, $\boldsymbol{a}$, $\boldsymbol{b}$, $\boldsymbol{s}_1, \ldots, \boldsymbol{s}_4$, $\boldsymbol{v}_1, \ldots, \boldsymbol{v}_4$.
2) Evaluation of the cylindrical functions: $J_m(\boldsymbol{k}^{\mathrm{s}}_{\perp 1,2} r^{\mathrm{s}})$, $J'_m(\boldsymbol{k}^{\mathrm{s}}_{\perp 1,2} r^{\mathrm{s}})$, $J_m(\boldsymbol{k}^{\mathrm{d}}_{\perp} r^{\mathrm{s}})$, $J'_m(\boldsymbol{k}^{\mathrm{d}}_{\perp} r^{\mathrm{s}})$, $N_m(\boldsymbol{k}^{\mathrm{d}}_{\perp} r^{\mathrm{s}})$, $N'_m(\boldsymbol{k}^{\mathrm{d}}_{\perp} r^{\mathrm{s}})$, $N_m(\boldsymbol{k}^{\mathrm{d}}_{\perp} R)$, $N'_m(\boldsymbol{k}^{\mathrm{d}}_{\perp} R)$, $H^{(2)}_m(\boldsymbol{k}^{\mathrm{a}}_{\perp} R)$, $H'^{(2)}_m(\boldsymbol{k}^{\mathrm{a}}_{\perp} R)$.
3) Calculation of the determinant elements: $\boldsymbol{a}_{jk}$ with $j = 0, 1, \ldots, 8$; and $k = 0, 1, \ldots, 8$.
4) Evaluation of the determinant: $D^{\mathrm{s}} = \det[\boldsymbol{a}_{jk}]$.

if $D^{\mathrm{s}} = 0$ then
write $h' r^{\mathrm{s}}$
write $f r^{\mathrm{s}}$
$h' r^{\mathrm{s}}(f r^{\mathrm{s}})$
end if

end for

C. Extraction of dispersion characteristics.

1) Initialization of the SLP NN structure [18].
2) Selection of the example set for SLP NN training.
3) Training of the SLP NN.
4) Classification of the waveguide dispersion characteristics modes.

D. Evaluation of the gyrotropic waveguide broad bandwidth.

1) Retrieval of the dispersion characteristic length l.
2) Linear approximation of the sets within three neighbouring nodes, Eq. (4).
3) Angle estimation between approximated line and $f r^{\mathrm{s}}$.
4) Evaluation of the lower cut-off frequency for selected dispersion characteristic (intersection between $k r^{\mathrm{s}}$ and approximated line with highest angle).

The created algorithm is tested when the relative permittivity tensor elements are $\mathrm{Re}(\boldsymbol{\varepsilon}^{\mathrm{s}}_{xx}) = \mathrm{Re}(\boldsymbol{\varepsilon}^{\mathrm{s}}_{zz}) = \varepsilon^{\mathrm{d}}_{\mathrm{r}} = 4$ and $\mathrm{Re}(\boldsymbol{\varepsilon}^{\mathrm{s}}_{xy}) = 0$. In this situation our proposed algorithm is adopted for dielectric waveguides analysis. In this case it is possible to compare dispersion characteristics with other authors' works [21, 22].

In Fig. 3 there are presented dispersion characteristics of dielectric waveguide when the radius of the dielectric waveguide is $r^{\mathrm{d}} = 10$ mm and azimuthal index $m = 1$ and $n = 1, 2, 3$. The dispersion characteristics obtained are the same as in [21, 22]. In comparison to the Kim [22] and Yeh [23] waveguide analysis methods, algorithm proposed in this paper is more flexible, as it gives the possibility to analyse the gyrotropic circular cylindrical waveguides.

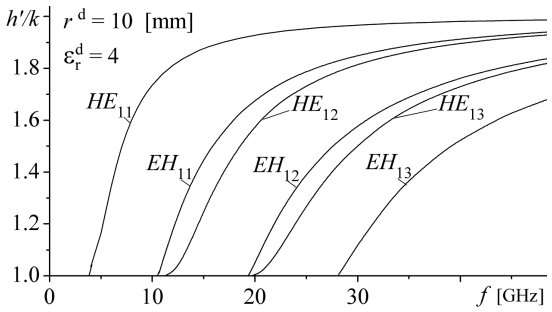

Fig. 3. The gyrotropic semiconductor waveguides analysis algorithm testing results, when $\varepsilon^{\mathrm{d}}_{\mathrm{r}} = 4$, $r^{\mathrm{d}} = 10$ mm, $m = 1$ and $n = 1, 2, 3$.

In Fig. 4 there are presented the n-InP gyrotropic waveguide dispersion equation roots — nodes of the waveguide modes. These nodes shout be grouped in order to retrieve the dispersion characteristics of the waveguide. In this paper a semi-automatic tool for classification of nodes dependent on the same mode is presented. The extraction of the dispersion characteristics (result is shown in Fig. 5) is made by sending all received data points (1, step 4 at the stage B, Fig. 4) to the trained SLP neural network. For waveguides electrodynamical parameters calculation it is necessary to extract only two types of dispersion characteristics: main mode HE_{11}, the first higher mode EH_{11} and the second higher mode HE_{12}. The other modes are less important and not used for further analysis. These modes are eliminated by the use of SLP NN and are not presented in Fig. 5 and Fig. 6.

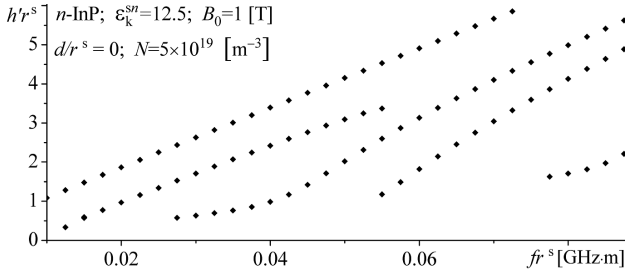

Fig. 4. Dispersion characteristics of the n-InP gyrotropic waveguides with total electron concentration $N = 5 \times 10^{19}$ m^{-3} and dielectric layer thickness is $d/r^{\mathrm{s}} = 0$, before extraction.

For the evaluation of waveguide broad bandwidth (algorithm 1, stage D) the linear approximation of the analysed dispersion characteristic is required [13, 14]. The linear approximation is performed by the following equation:

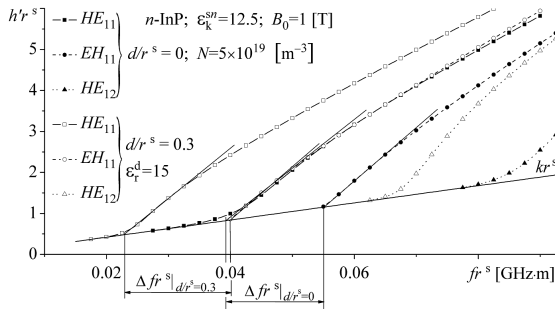

Fig. 5. Dispersion characteristics of the n-InP gyrotropic waveguides with total electron concentration $N = 5 \times 10^{19}$ m^{-3} extracted with the use of SLP NN.

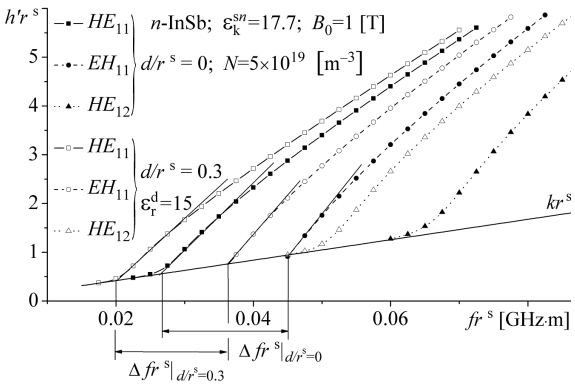

Fig. 6. Dispersion characteristics of the n-InSb gyrotropic waveguides with total electron concentration $N = 5 \times 10^{19}$ m^{-3} extracted by the SLP NN.

$$\boldsymbol{c} = \frac{\boldsymbol{A}_1' \boldsymbol{A}_1}{\boldsymbol{A}_1' \boldsymbol{H}_1}\,, \tag{4}$$

where $\boldsymbol{c}$ is the vector of the line equation $y = c_1 x + c_2$; coefficients c_1 and c_2, coefficients $\boldsymbol{A}_1' \boldsymbol{A}_1$ and $\boldsymbol{A}_1' \boldsymbol{H}_1$ are the results of fr_t^{s} and $h'r_t^{\mathrm{s}}$ written in matrix form.

Normalized working frequencies of the waveguides in the range Δfr^{s} were established as the difference between cut-off frequency $f_{\mathrm{cut}1} r^{\mathrm{s}}$ of the first higher mode EH_{11} and a cut-off frequency $f_{\mathrm{cut}0} r^{\mathrm{s}}$ of the main mode HE_{11} [13, 14]. The broad bandwidth of the waveguide is calculated using the following expression:

$$\delta_f^{\mathrm{s}} = \frac{\Delta fr^{\mathrm{s}}}{f_{\mathrm{c}} r^{\mathrm{s}}} \times 100[\%] = \frac{2(f_{\mathrm{cut}1} - f_{\mathrm{cut}0}) r^{\mathrm{s}}}{(f_{\mathrm{cut}1} + f_{\mathrm{cut}0}) r^{\mathrm{s}}} [\%]\,, \tag{5}$$

where $f_{\mathrm{c}} r^{\mathrm{s}}$ is the normalized central frequency of the waveguide working frequency range.

4. Analysis of different type gyrotropic semiconductor waveguides

Three types of gyrotropic circular cylindrical waveguides are analysed in this paper. First type of the semiconductor waveguides is n-InP, the second type is n-InSb and the third type is p-InP. In this chapter the broad bandwidths of the n-InP and p-InP circular cylindrical semiconductor, semiconductor–dielectric waveguides are compared. Furthermore, the semiconductor, semiconductor–dielectric waveguides electrodynamics parameters are presented. The dispersion characteristics are calculated for the analysed types of waveguides with radius $r^{\mathrm{s}} = 1$ mm and with hybrid modes first (azimuthal) index $m = 1$. The algorithm presented in this paper uses normalized phase constant $h'r^{\mathrm{s}}$ dependences on the normalized frequency fr^{s} to calculate the waveguides broad bandwidth, working frequency range (see Fig. 5 and Fig. 6), cut-off frequencies of the modes and central working frequency. The polarization of the hybrid modes is left-hand $\exp(+\mathrm{i}m\phi)$.

A mistyping mistake in [19] is corrected in this paper. The types of waveguide are taken from n-InP instead of p-InP (as noted in paper [19]). The dispersion characteristics of the semiconductor waveguide are presented in Fig. 5 and Fig. 6. Here the mode HE_{11} is denoted with square markers, the higher mode EH_{11} is denoted with circle markers and the second higher mode HE_{12} is denoted with triangle markers in the figure. The analysis of the semiconductor n-InP waveguides is performed by taking material background dielectric constant $\varepsilon_k^{sn} = 12.5$. Effective mass of the n-InP semiconductor electron is $m^* = 0.08 m_{\mathrm{e}}$ and mobility $\mu = 5.4$ m^2 V^{-1} s^{-1}, here m_{e} is mass of free carrier [24]. Dispersion characteristics of the waveguides are presented in Fig. 5. For these calculations the dielectric TM15 is used. The relative permittivity of selected dielectric is $\varepsilon_{\mathrm{r}}^{\mathrm{d}} = 15$ and a relative (normalized) thickness is $d/r^{\mathrm{s}} = 0.3$.

n-InP semiconductor waveguides working frequency range is $\Delta fr^{\mathrm{s}}|_{d/r^{\mathrm{s}}=0} = 0.016$ GHz m and broad bandwidth $\delta_f^{\mathrm{s}} = 34\%$, semiconductor–dielectric waveguides working frequency range is $\Delta fr^{\mathrm{s}}|_{d/r^{\mathrm{s}}=0.3} = 0.018$ GHz m. For this type of waveguides, the broad bandwidth increases for about 24% and becomes $\delta_f^{\mathrm{s}} = 58\%$. It means that the cut-off frequencies of the modes HE_{11}, EH_{11} moves to lower frequencies. The cut-off frequency HE_{11} of the main mode without external dielectric layer is $f_{\mathrm{cut}0} r^{\mathrm{s}}|_{d/r^{\mathrm{s}}=0} = 0.039$ GHz m. Together with external dielectric layer the main mode HE_{11} cut-off frequency $f_{\mathrm{cut}0} r^{\mathrm{s}}$ is moving about 0.017 GHz m to lower the side of frequencies.

When the external dielectric layer is added to the waveguide, the cut-off frequencies of the main mode HE_{11} always move to lower frequencies side because external dielectric layer changes the electromagnetic field structure in gyrotropic waveguides core.

n-InSb gyrotropic waveguides analysis is performed with material background dielectric constant $\varepsilon_k^{sn} = 17.7$ [13]. Effective mass of the n-InSb semiconductor electron is $m^* = 0.013 m_{\mathrm{e}}$ with the mobility of $\mu = 7$ m^2 V^{-1} s^{-1}. Dispersion characteristics for the n-InSb semiconductor, semiconductor–dielectric waveguides are presented in Fig. 6.

The dispersion characteristic shows that the external dielectric layer changes semiconductor and

semiconductor–dielectric waveguides working frequency range and broad bandwidth. Semiconductor--dielectric n-InSb waveguides working frequency range is $\Delta fr^{\mathrm{s}}|_{d/r^{\mathrm{s}}=0.3} = 0.016$ GHz m. With external dielectric layer semiconductor n-InSb waveguides broad bandwidth is $\delta_f^{\mathrm{s}} = 57.1\%$. The working frequency range is smaller than n-InP semiconductor–dielectric waveguides working frequency range.

n-InSb semiconductor waveguides working frequency range is $\Delta fr^{\mathrm{s}}|_{d/r^{\mathrm{s}}=0} = 0.018$ GHz m and broad bandwidth is $\delta_f^{\mathrm{s}} = 50\%$. Without external dielectric layer n-InSb waveguides broad bandwidth is wider compared to n-InP gyrotropic waveguides broad bandwidth. Difference between these two types of waveguides broad bandwidths is about 16% (about 1.47 times). According to the analysis results, the use of n-InSb waveguides is preferable for production because their electrodynamical parameters (broad bandwidth and working frequency range) are better, comparing to n-InP waveguides, when the electron concentration is $N = 5 \times 10^{19}$ m^{-3}.

Next, the investigation results of the n, p-InP semiconductor, semiconductor–dielectric waveguides characteristics are presented in the paper. The thickness of the external dielectric layer is changed $d/r^{\mathrm{s}} = 0$, 0.1, 0.2, 0.3, 0.4, 0.5, also the concentrations of free carrier, used for the analysis are $N = 1 \times 10^{17}$, 5×10^{18}, 5×10^{19}, 1×10^{20} m^{-3}.

p-InP gyrotropic waveguides main electrodynamical properties are: effective mass of the free carrier $m_\Sigma^* = 0.58 m_{\mathrm{e}}$, the mobility $\mu_\Sigma^* = 0.02$ m^2 V^{-1} s^{-1}, the material background dielectric constant (the same as n-InP waveguides).

Broad bandwidth dependences on the free carrier concentration ($\lg N$) and the dielectric layer thickness (d/r^{s}) are presented in Fig. 7. It can be seen that increasing the concentration of the free carrier of the waveguides, the broad bandwidth δ_f^{s} does not change. The waveguides broad bandwidth changes only when the external dielectric layer is used. The widest p-InP gyrotropic waveguides broad bandwidth ($\delta_f^{\mathrm{s}} = 68.3\%$) is received when the normalized thickness of the dielectric layer is $d/r^{\mathrm{s}} = 0.5$. The narrowest waveguides broad bandwidth is received with dielectric layer thickness $d/r^{\mathrm{s}} = 0.2$. Consequently, with this dielectric layer thickness waveguide's broad bandwidth decreases to $\approx 4\%$ and becomes $\delta_f^{\mathrm{s}} = 64.3\%$. It happens because p-InP semiconductor and semiconductor–dielectric waveguides, effective mass of the free carrier and mobility are very small. These results are important for designing various microwave devices, such as phase shifters.

More interesting results of investigation are received for the n-InP semiconductor and semiconductor–dielectric waveguides. These results are shown in Fig. 8. It can be seen that n-InP gyrotropic waveguides broad bandwidth varies when the electron concentration is increasing. Also the waveguides broad bandwidth increases if the external dielectric layer thickness d/r^{s} is increasing as well.

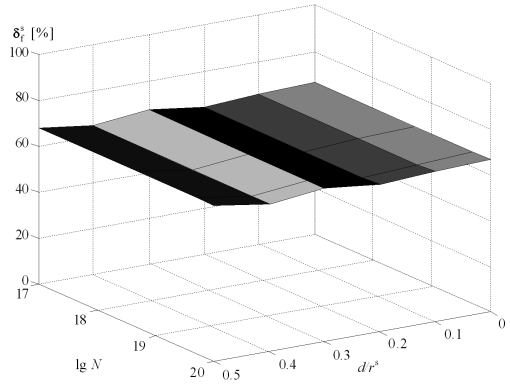

Fig. 7. p-InP gyrotropic waveguides broad bandwidth dependences on the free carrier concentration and the dielectric layer thickness.

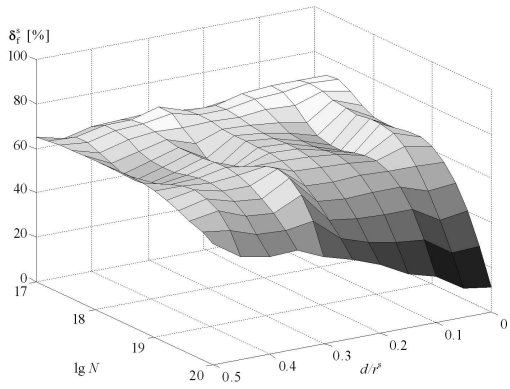

Fig. 8. n-InP gyrotropic waveguides broad bandwidth dependences on the electron concentration and the dielectric layer thickness.

The widest n-InP semiconductor, semiconductor–dielectric waveguides broad bandwidth is received for waveguides with electron concentration $N = 5 \times 10^{18}$ m^{-3} and normalized thickness of the dielectric layer equal to 0. The broad bandwidth of evaluated waveguides is $\delta_f^{\mathrm{s}} = 68.9\%$.

Increasing the thickness of the dielectric layer, waveguides broad bandwidth also increases if the electron concentration is $N = 1 \times 10^{20}$ m^{-3}. The n-InP gyrotropic waveguides broad bandwidth will be $\delta_f^{\mathrm{s}} = 67.3\%$, when the electron concentration is $N = 5 \times 10^{18}$ m^{-3} and external dielectric layer's thickness is $d/r^{\mathrm{s}} = 0.5$.

Without external dielectric layer n-InP gyrotropic waveguides broad bandwidth is $\delta_f^{\mathrm{s}} \approx 11\%$, with electron concentration it is $N = 1 \times 10^{20}$ m^{-3}.

It can be seen in Fig. 8 that the increasing concentration of the electrons in the n-InP gyrotropic waveguides the broad bandwidths for different modes are decreasing, because of the cyclotron resonance frequency effects.

All these calculation results are significant and can be used for designing and manufacturing microwave devices. The differences between phases in semiconductor

and semiconductor–dielectrics waveguides regarding the phase shifters have been calculated.

5. Conclusions

According to the investigation results the external dielectric layer changes the structure of gyrotropic semiconductor waveguide's core electromagnetic field. Increasing dielectric layer thickness, the broad bandwidth of the waveguide is increasing when electron concentration is $N = 1 \times 10^{20}$ m^{-3}, for the n-InP waveguides.

n-InP and p-InP waveguides are better than n-InSb gyrotropic semiconductor, semiconductor–dielectric waveguides, when free carrier concentration is $N = 5 \times 10^{19}$ m^{-3} and external dielectric layer thickness is $d/r^{s} = 0.3$. n-InP and p-InP waveguides broad bandwidths are wider than n-InSb.

p-InP semiconductor, semiconductor–dielectric waveguides broad bandwidth does not depend on the free carrier concentration. The free carrier mobility μ^{*}_{Σ} of the p-InP waveguide is very small compared to the n-InP waveguide electrons mobility.

The use of SLP NN enables to extract linear separable dispersion characteristics of the gyrotropic semiconductor and semiconductor–dielectric waveguide from the set of computed nodes quickly. Using a proposed semi-automatic analysis of algorithm it is possible to quickly evaluate the cut-off frequencies for different waveguides modes, the waveguide working frequency range and the broad bandwidth.

References

[1] N. Zaitsev, I. Kulagin, S. Kuzikov, M. Plotkin, I. Syratchev, in: *Infrared and Millimeter Waves, 2007 and the 15-th International Conference on Terahertz Electronics, IRMMW-THz, Joint 32nd Int. Conf.*, Eds. M.J. Griffin, P.C. Hargrave, T.J. Parker, K.P. Woo, Institute of Electrical and Electronic Engineer, Cardiff (UK) 2007, p. 369.

[2] D. Loik, M. Nefedov, E. Nikishin, in: *Actual Problems of Electron Devices Engineering, 2008, APEDE' 08, Int. Conf.*, Ed. V.A. Tsarev, publisher: Saratov State Technical University, Saratov (Russia) 2008, p. 324.

[3] M. Yeddulla, S. Tantawi, J. Guo, V. Dolgashev, *Microwave Theory Techn.* **6**, 57 (2009).

[4] C.W. Yuan, Q. Zhang, *Plasma Sci.* **10**, 37 (2009).

[5] G. Gentili, L. Lucci, R. Nesti, G. Pelosi, S. Selleri, *Microwave Theory Techn.* **7**, 57 (2009).

[6] M. Dillon, A. Gibson, J. Webb, *Microwave Theory Techn.* **5**, 41 (1993).

[7] D.M. Sullivan, *Electromagnetic Simulation Using the FDTD Method*, Institute of Electrical and Electronics Engineers, New York 2000.

[8] L. Nickelson, V. Shugurov, *Singular Integral Equations' Methods for the Analysis of Microwave Structures*, VSP Publishing Int. Sci. Publ., Leiden 2005.

[9] B.J. Hu, G. Wei, *Plasma Sci.* **1**, 29 (2001).

[10] N. Dib, A. Omar, *Microwave Theory Techn.* **7**, 50 (2002).

[11] D. Rovetta, A. Bosisio, G. Drufuca, *Microwave Wireless Components Lett.* **5**, 16 (2006).

[12] S. Asmontas, L. Nickelson, V. Malisauskas, *Electron. Electr. Eng.* **2**, 66 (2006).

[13] L. Nickelson, S. Asmontas, V. Malisauskas, V. Sugurovas, *Open Cylindrical Gyrotropic Wavequides*, Technika, Vilnius 2007.

[14] L. Nickelson, S. Asmontas, V. Malisauskas, R. Martavicius, *Plasma Phys.* **1**, 75 (2008).

[15] D. Navakauskas, *Informatica* **2**, 14 (2003).

[16] S. Paulikas, D. Navakauskas, *Informatica* **2**, 17 (2006).

[17] D. Matuzevicius, D. Navakauskas, in: *Proc. 11th Int. Biennial Baltic Electronics Conf.*, Ed. J. Engelbrecht, Tallinn University of Technology, Tallinn (Estonia) 2008, p. 341.

[18] F. Rosenblatt, *Principles of Neurodynamics: Perceptrons and the Theory of Brain Mechanisms*, Spartan Books, Washington 1962.

[19] D. Plonis, V. Malisauskas, A. Serackis, in: *Microwave Radar and Wireless Communications (MIKON), 2010 18th Int. Conf.*, Ed. B. Levitas, Geozondas, Vilnius (Lithuania) 2010, p. 508.

[20] E.D. Palik, J.K. Furdyna, *Rep. Prog. Phys.* **12**, 33 (1970).

[21] L. Nickelson, T. Gric, S. Asmontas, R. Martavicius, *Electron. Electr. Eng.* **2**, 82 (2008).

[22] K.Y. Kim, H.S. Tae, J.H. Lee, *Electron. Lett.* **39**, 61 (2003).

[23] C. Yeh, F.I. Shimabukuro, *The Essence of Dielectric Waveguides*, Springer Science, Business Media, USA 2008.

[24] S.M. Sze, *Physics of Semiconductor Devices*, Wiley, USA 1981.